

Polymeric ionic liquid—assisted polymerization for soluble polyaniline nanofibers

Jie Liu^{1*}, Jiahao Shen^{1*}, Jingjing Wang¹, Yuan Liang¹, Routeng Wu¹, Wenwen Zhang¹, Delin Shi², Saixiang Shi², Yanping Wang¹, Yimin Wang¹, Yumin Xia (✉)¹

¹ Key Laboratory of High Performance Fibers & Products (Ministry of Education), State Key Laboratory for Modification of Chemical Fibers and Polymer Materials, College of Science, College of Materials Science and Engineering, Donghua University, Shanghai 201620, China
² Hunan Changsha Aiwaning Home Textile Products Co. Ltd, Changsha 410600, China

© Higher Education Press 2021

Abstract To enhance the solubility of polyanilines (PANI), polymeric ionic liquid (PIL) was introduced into the polymerization synthesis of PANI with various proportions. The structure and properties of the modified PANIs were characterized by ¹H NMR, Fourier transform infrared spectroscopy, thermogravimetric analysis, ultraviolet-visible spectrum, etc. It was found that the obtained PANIs doped with PILs were soluble in various organic solvents such as *N,N*-dimethyl formamide and acetonitrile. Compared with the pure PANI, the PANIs doped by PILs showed remarkable solubility and their chemical structure and conductivity kept integrated.

Keywords polyaniline, polymeric ionic liquid, doping, solubility

1 Introduction

Polyaniline (PANI) is a conducting polymer in the semi-rigid rod polymer family, and has great potential application in conductive and antistatic materials, sensors and stealth materials, etc. [1–7]. Recently, as the fast development of smart materials in optical and electrical research field, polyaniline has attracted much more attention due to its excellent properties such as environmental stability, convenient synthesis, tunable properties and low production cost, and is always combined with organic and inorganic materials to fabricate novel form of composites [8,9].

However, the processability of PANI still remains a

significant challenge. PANI is hardly able to dissolve or melt and this limits its practical application [10]. Fundamentally, the poor solubility and high melting point of polyaniline are mainly due to the conjugate nature of its π -electronic structure and strong coulomb interactions [11]. Various methods were used to enhance its processability based on the unique chemical structure of PANI [12–15]. It has been reported that PANI can be doped by many surfactants for better solubility [16–18]. For example, acids with bulky organic anion, such as *d,l*-camphorsulfonic acid and dodecyl benzene sulfonic acid, were doped into PANI, and obtained PANI can be dispersed in organic solvents such as *m*-cresol and chloroform [19,20]. The improvement of solubility was attributed to the bulky organic anions which can effectively decrease coulomb interactions between PANI chains and allow the penetration of solvent molecules into the polymer chains. Meanwhile the inter-chain interactions among the conjugated PANI chains can be isolated by the attaching side chains in the bulky organic anion [21]. The methods mentioned above were all based on the coulomb interactions between the cation and anion structure. On the other hand, π -conjugated structure is another significant feature of PANI which provides a promising approach to enhance the solubility of PANI [22].

Carbon materials including graphene and carbon nanotube also have π -conjugated structure, and they are all insoluble and difficult to disperse in common solvents as the PANI did. Polymeric ionic liquids (PILs) as novel polymers have drawn much attention in recent years. PILs contain ionic liquid (IL) moieties either in their backbone or side chains, and combine attractive IL properties, showing potential applications in ionic conductors, absorbents, and catalysts [23–26]. Especially, PILs were reported as dispersants for graphene and carbon nanotubes in many solvents. For example, Marcilla et al. reported the

Received October 21, 2019; accepted December 15, 2019

E-mail: xym@dhu.edu.cn

*These authors contributed equally to this work.

synthesis of PIL poly(1-vinyl-3-ethylimidazolium bromide) and used it to stabilize the carbon nanotubes in water [25]. Schüler et al. reported a kind of hyperbranched PIL C18hyperImOTs which was a highly effective dispersing agent for graphene. In the presence of C18hyperImOTs, stable graphene dispersions were formed in nonpolar media, such as toluene, whereas dispersions of graphene in pure toluene underwent rapid sedimentation [26]. Kim et al. reported chemically converted graphene sheets modified with PIL were stable to the chemical reduction and could be well dispersed in the aqueous phase without any agglomeration. It could be attributed to the π -cation interaction between the carbon material and the imidazole group of PIL, and this specific interaction makes PIL a promising agent to the dispersion of these π -conjugated structure materials [27,28].

Since the PIL were used to enhance the solubility of carbon materials which had the similar π -conjugated structure of PANI, we improved the solubility of PANI with the assistance of PIL. A kind of PIL (PIL-Cl) was designed and synthesized, and this PIL contains a cationic imidazole group and an anionic chlorine group on the side chain. Then this PIL was introduced during the polymerization process of PANI. PILs can strongly interact with π -conjugated structure and significantly improve the solubility of PANI. The performance of PIL-doped samples with different mass ratios was compared. The results showed that PIL could significantly improve the solubility of PANI, which is particularly important for broadening the application of PANI.

2 Experimental

2.1 Materials

Aniline (ANI, 99%, Aladdin Reagent (Shanghai) Co., Ltd, AR), ammonium persulfate (APS, 99%, Sinopharm Chemical Reagent Co., Ltd, AR), and HCl (37%) were used as received without further purification. Phthalic anhydride (Sinopharm Chemical Reagent Co., Ltd, AR) was dried under vacuum at 70°C for 24 h before use. Epichlorohydrin (ECH, Sinopharm) and *N,N*-dimethyl formamide (DMF, Sinopharm) were stirred with CaH₂ and then distilled under vacuum prior to use. *N*-Methylimidazole (99%, damas-beta, China) and acetone were used as received. The solvents, dimethyl sulfoxide (DMSO) and *N,N*-dimethylacetamide (DMAc), in analytical grade reagents were purchased from Sinopharm Chemical Reagent Co., Ltd. and used as received.

2.2 Synthesis

The synthetic method of PIL-Cl was followed reference [29], and a typical synthetic process was described in supporting information. Polyaniline was synthesized as

follows: 40 mmol ANI was added slowly to 136.4 mL HCl (1.44 mol/L) solution under fiercely magnetic stirring condition for 10 min to form an aqueous phase solution. Meanwhile, 0.93 g (4.08 mmol) APS dissolved in 40 mL H₂O was added into the reaction system and stirred at 25°C for 2 h. The obtained dark green samples were washed by acetone for three times and dried at 40°C for 24 h in vacuum-oven. The product obtained was named PANI.

Polyaniline doped by PILs was prepared as follows: 4.08 mmol APS dissolved in 40 mL H₂O in the flask. 40 mmol ANI (3.72 g) was first mixed with 0.93 g, 1.24 g, 1.86 g PIL-Cl (Table 1) respectively, and then the mixtures were added slowly into the 136.4 mL HCl (1.44 mol/L) solution in the flask. After stirring for 2 h at 25°C, these 4 samples were obtained by precipitation and washed with acetone for 3 times. Then these samples were named according to the complex ratio for PIL-Cl and PANI which could be calculated with the percentages of residuals at 450°C in TG spectra analysis, as showed in Table 2.

Table 1 Weight ratio for polymerization of PANI doped by PIL-Cl

Sample	Sample 1	Sample 2	Sample 3	Sample 4
Weight of PIL-Cl/g	0	0.93	1.24	1.86
Weight ratio of PIL-Cl to ANI	0	1:4	1:3	1:2

Table 2 The complex information of each samples under different reaction ratios

Materials ratio	Weight loss/%	Complex ratio		Sample name
		PIL-Cl/%	PANI/%	
1:0	85.4	–	–	PIL-Cl
1:2	46.5	46.5	53.5	PANI-PIL3
1:3	25.3	17.4	82.6	PANI-PIL1
1:4	34.1	29.5	70.5	PANI-PIL2
0:1	12.6	–	–	PANI

PANI/Graphene with PILs was synthesized as follows: APS (4.08 mmol) was dissolved in 40 mL H₂O in the flask. ANI (3.72 g, 40 mmol) mixed with 1.24 g PIL-Cl and 1.24 g graphene was added slowly into the flask at the same time as the 136.4 mL HCl (1.44 mol/L) solution. After polymerization at 25°C for 2 h, the sample was obtained by precipitation and washing with acetone, and dried at 40°C for 24 h in vacuum-oven. The product was named PANI-PIL-G.

2.3 Characterization and measurement

¹HNMR spectra were obtained on a Bruker Avance 400 NMR spectrometer (Bruker BioSpin AG, Switzerland) at 300 MHz with DMSO-d₆ as solvents at room temperature. Fourier transform infrared spectroscopy (FTIR) was

performed with KBr pellets on a Nicolet 8700 infrared spectrum analyzer in a test range of $4000\text{--}550\text{ cm}^{-1}$. X-ray photoelectron spectroscopy (XPS) analysis was carried out on Escalab 250Xi instrument using a monochromatized Al KR X-ray source (1486.71 eV photons). Thermogravimetric analysis (TGA) was conducted by using a Netzsch TG 209 F1 from 100°C to 50°C with a constant rate of $20^\circ\text{C}/\text{min}$ in nitrogen atmosphere. Ultraviolet-visible spectra (UV-Vis) were recorded in the wavelength range of $250\text{--}800\text{ nm}$ at room temperature, using Lambda 35 UV-Vis spectrometer (Perkin Elmer, USA). Each sample was dissolved in DMF. The X-ray diffraction (XRD) patterns were recorded by the Bruker AXS Generator with a nickel filtered Cu-K α radiation at 40 kV and 30 mA , by the Cu-K α monochromatic radiation with a wavelength of 0.154 nm . The powder samples were measured using a flat sample holder in reflection mode with their scans recorded in the 2θ range of $5^\circ\text{--}60^\circ$. The surface morphology was investigated by using scanning electron microscopy (SEM) (JSM-5600LV; JEOL, Japan). The microstructure of particles was observed with transmission Electron Microscope (TEM) (JEOL JEM-2100). The electrical conductivity was measured using SDY-4 Four-Point Probe Meter at 25°C . The pellets were prepared by subjecting the powder sample to a pressure of 30 MPa .

3 Results and discussion

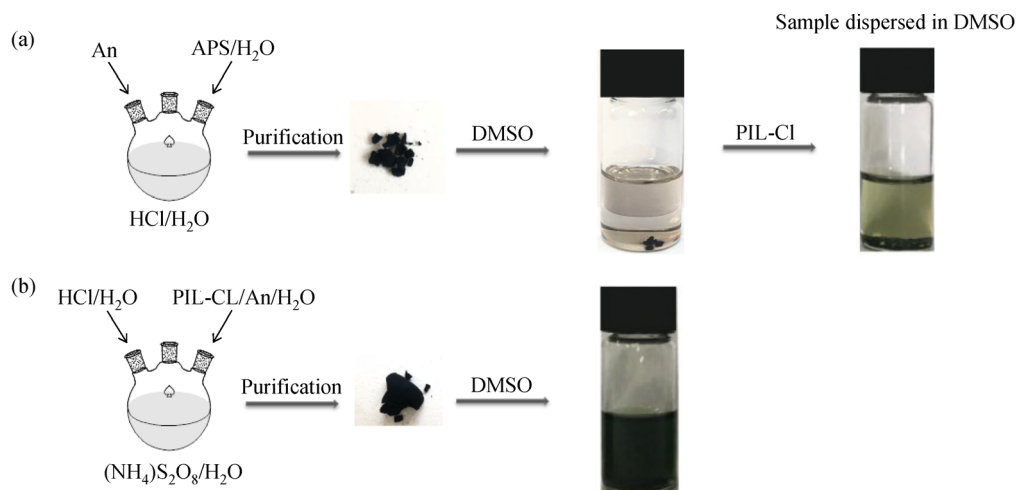
3.1 Synthesis of polyaniline doped by PILs

In present experiment, the PILs-doping PANIs were synthesized by introducing PIL during the polymerization of PAN, meanwhile unmodified PANI was also synthesized by traditional method. As showed in Scheme 1(a), the solubility experiment showed that the unmodified

PANI couldn't be dispersed well in DMSO with or without PIL-Cl. This may be caused by the aggregation of PANI during the polymerization. Therefore, we designed an improved synthetic method to dope PILs into PANI during the polymerization. In detail, the monomer ANI was mixed with PIL-Cl aqueous solution first, and added into the flask which had APS solution in the bottom. After stirring for 2 h , the reaction solution was precipitated in acetone and washed several times to obtain the product PANI-PIL (PIL-doped PANI). The product has the same color as pure PANI and it can be well dispersed in DMSO (Scheme 1(b)). This result demonstrated that PILs (PIL-Cl) can improve the dispersion of PANI when it was introduced into the polymerization of PANI. Furthermore, three PANI-PIL samples with different weigh ratios of PIL-Cl to ANI were synthesized according to the improved synthetic procedure, and their chemical and physical properties were characterized and compared with pure unmodified PANI.

3.2 Morphologies and dispersing behavior of PANI doped by PILs

The SEM images of pure PANI and those PANIs doped by different weight ratios of PIL-Cl (PANI-PIL) were presented in Fig. 1, respectively. It showed that the pure PANI had one-dimensional radially aligned nanofiber structures, which are highly tangled with each other with a smooth surface [14]. Compared with pure PANI, SEM images of PIL-doped PANI (PANI-PIL) show mixed morphology, in which cloud-like morphology is mixed with nanoparticles, indicating that PIL-Cl encapsulates pure PANI and influence the formation of the surface morphology. Otherwise, these four samples showed tiny difference on morphology due to the ratio of PIL-Cl. Corresponding to the SEM images, the TEM images as



Scheme 1 Comparison of the sample (a) doping PIL-Cl after the polymerization of PANI and (b) doping PIL-Cl during the polymerization of PANI.

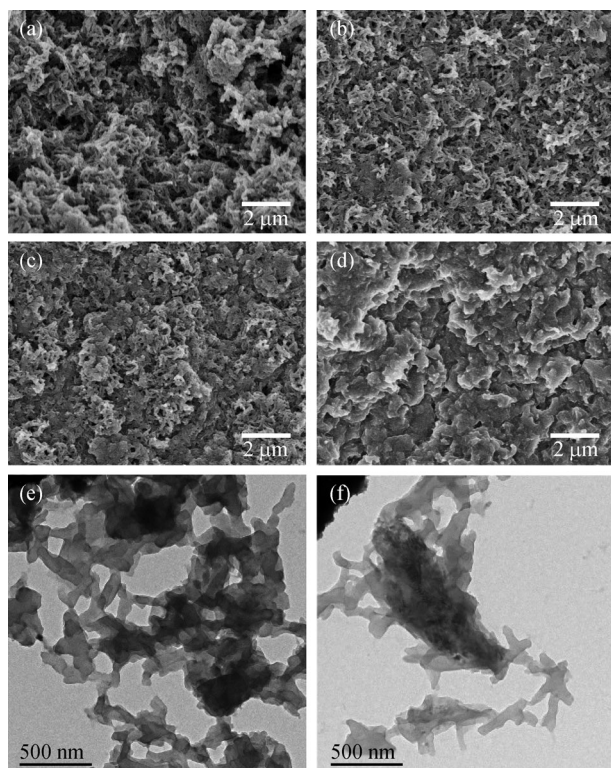


Fig. 1 SEM image of (a) the pure PANI, (b) PANI-PIL1, (c) PANI-PIL2, (d) PANI-PIL3 and TEM image of (e) PANI-PIL1, (f) PANI-PIL3.

presented in (e) and (f), showed the same one-dimensional radially aligned nanofiber structure, it could be concluded that the structure of PANI retains the doping of PIL-Cl.

In the PANIs solubility experiment (Fig. 2), the concentration of the PANIs dispersion in water, DMSO, DMAc and DMF was fixed at 1 mg/mL. After shaking and sonication, the supernatant liquid phase of pure PANI

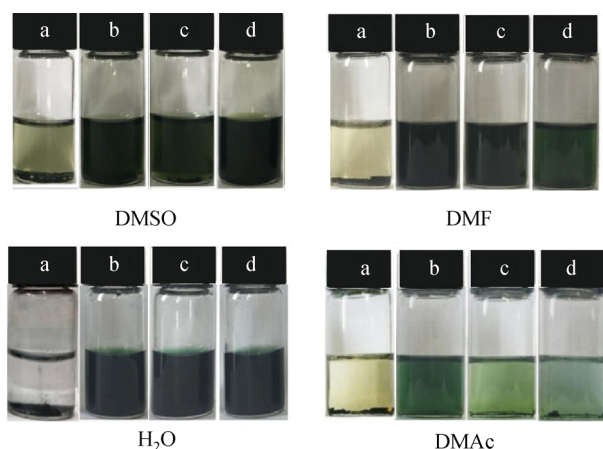


Fig. 2 Solubility experiments of (a) the pure PANI, (b) PANI-PIL1, (c) PANI-PIL2 and (d) PANI-PIL3 dispersed in water, DMSO, DMAc and DMF.

retained clear and colorless, while the liquid phase of PANI doped with PILs became turbid. This phenomenon indicates that the PANIs could be dispersed well in water, DMSO, DMAc and DMF phase, while pure PANI couldn't. This is because during the polymerization, the quinoid moiety in the PANI and imidazolium ring in PIL formed π - π interaction between PANI and PILs [30]. This strong interaction made the PIL able to assist the PANIs chain dispersing in the most solvent.

3.3 Characterization of PANI doped by PIL-Cl

The chemical structures of PANI-PILs were characterized by $^1\text{H-NMR}$, FTIR, UV-Vis and XPS. In $^1\text{HNMR}$ spectra (Fig. 3(A)), it can be seen that the new signal from PIL-Cl appeared in the spectra compared with that of the pure PANI. The signal at 4.29–4.89 ppm was attributed to the protons from the methylene group connected to the carbonyl. The signal for the carbonyl was located at 5.76 ppm. The peak at 9.18–9.70 ppm belonged to the proton in the methine connected with the two nitrogen atoms, while other proton peaks of the imidazole ring were overlapped with the benzene ring at 7.49–8.07 ppm. This confirmed that the structure of polymeric ionic liquid PIL-Cl existing in the obtained composites. To further confirm the structures of the obtained polymers, the FTIR spectra were used to characterize those PANIs and presented in Fig. 3(B). It could be observed that the typical PANI structure peaks are presented at 1566 and 1472 cm^{-1} due to the C=C stretching vibration of quinoid and benzenoid ring, attributing to the N=Q=N and N-B-N groups [8]. This indicated these composites maintain the chemical structure of PANI. XPS spectra of doped PIL-Cl and pure PANI were shown in Fig. 4. The high-resolution XPS in the N 1s region indicated that it existed three different electronic states: benzylamine with binding energy (BE) centered at 399.7 eV, the quinoid amine with BE at 399.0 eV, and the nitrogen cationic radical (N^+) with BE at 401.4 eV. After doped with PIL-Cl, a new peak centered at 398.5 appeared. At the same time, the peak of nitrogen cationic radical enhanced. This was attributed to the two different nitrogen atoms in imidazolium of PIL-Cl [31,32].

Figure 5(A) shows the Raman spectrum of PANI and PANI3. The characteristic bands at 1176 and 1380 cm^{-1} were assigned to C-H in plane bending of the quinoid rings and C-N stretching of benzenoid rings, respectively. The band at 1506 cm^{-1} was assigned to C=N stretching from the protonated quinoid diimine units of the doped PANI. An important feature could be observed in the Raman spectra: the characteristic C=N stretching band of the PANI quinoid segments of PANIPIIL was at 1474 cm^{-1} , while in pure PANI samples, this mode appears at 1506 cm^{-1} . This shift indicated the change in the torsion angle of quinoid benzenoid segments of PANI, which was due to the interaction between PANI and PIL-Cl [33]. It could be concluded that these composites maintain the

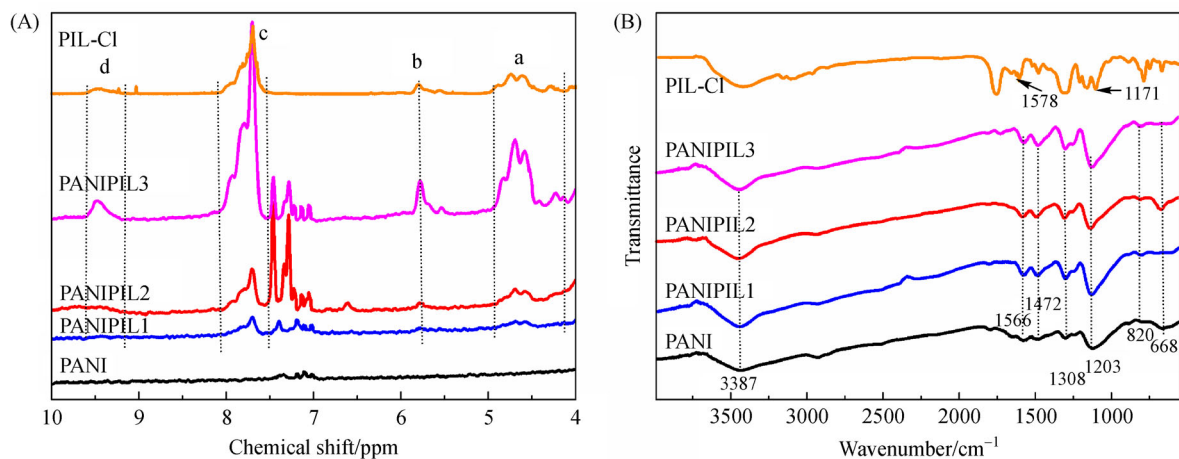


Fig. 3 $^1\text{H NMR}$ and FTIR spectra of the pure PANI, PANIPIL1, PANIPIL2, PANIPIL3 and PIL-Cl.

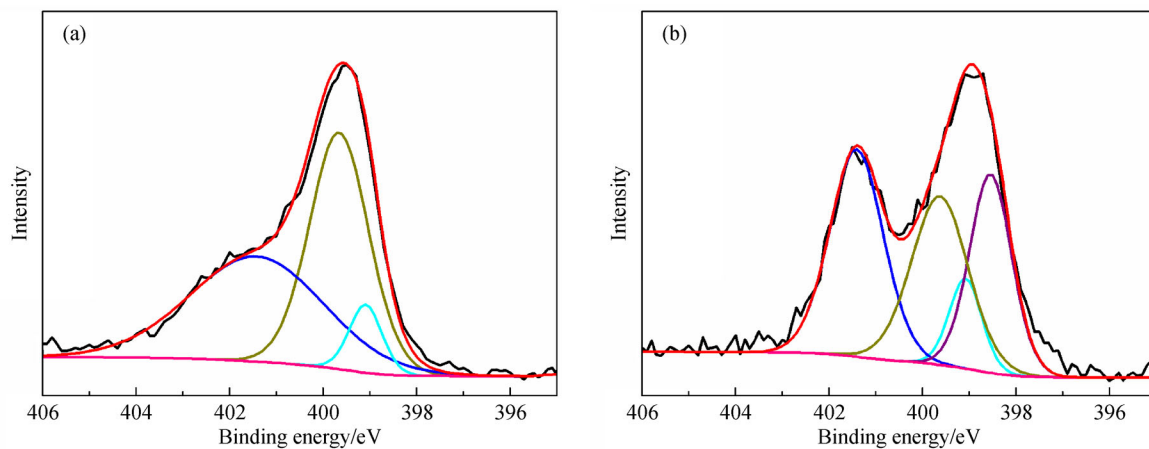


Fig. 4 N 1s region in XPS spectra of the (a) pure PANI and (b) PANIPIL1.

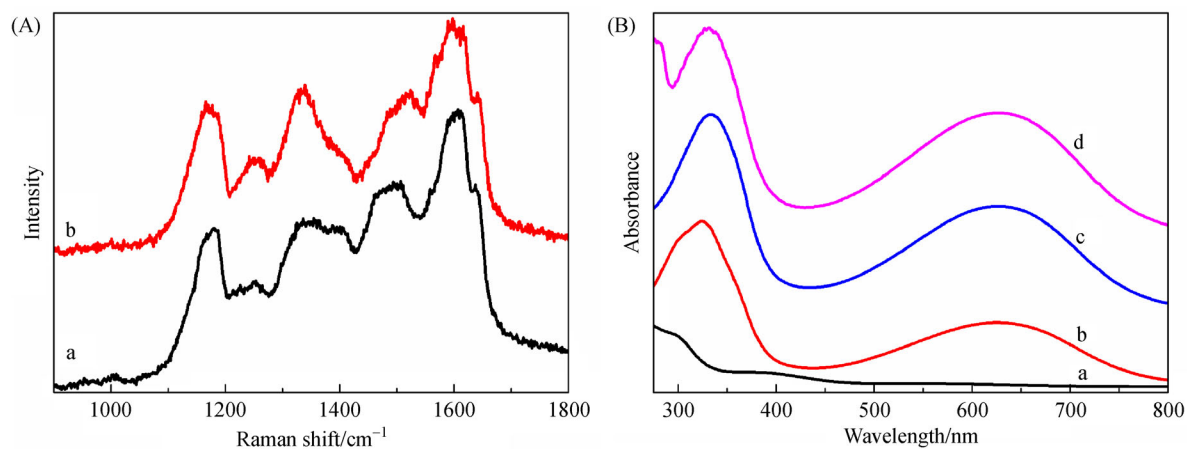


Fig. 5 (A) Raman spectroscopy of (a) the pure PANI and (b) PANIPIL1; (B) UV spectroscopy of (a) the pure PANI, (b) PANIPIL1, (c) PANIPIL2 and (d) PANIPIL3.

structure of the PANI and PIL-Cl respectively, and the interaction between PANI and PIL was non-covalent. The UV-Vis spectra of those 4 PIL-Cl doped and pure PANIs were showed in Fig. 5(A). The typical UV peaks for PANI were located at 309 and 603 nm due to the π - π^* and n - π transition corresponding to the benzene and quinone units vibration, respectively [15]. It could be observed that these two peaks were shifted in the PIL doped PANIs, e.g., at 340 and 640 nm. These dopant-induced quinone related structure in these PANIs were in good agreement with literature [34], indicating that the PANI doped with PIL-Cl would lead the atoms of both H^+ and N to form the conjugate structure within the PANI chains. Comparing spectra of these three PANIs doped with PIL-Cl, the peaks located at the same position, which suggested that doping PIL-Cl in PANI had no significant influence on chemical structure of PANI.

3.4 Thermal property of PANI doped by PILs

The TGA curves of pure PANI and doped PANIs were shown in Fig. 6. The weight losses below 100°C represented the evaporation of imbibed water. It was observed that all of these samples presented three thermal degradation stages, and this was consistent with the literature [8]. Moreover, the thermal stabilities of PANIs were compared with the pure PIL-Cl in Fig. 6. It could be found that in the second temperature heating stage (about 250°C–300°C), the weight loss was visibly for the doped PANIs compared to the pure PANI. This was because the degradation of PANI. In the meantime, it was also found that at about 100°C–220°C, the weight loss of doped PANIs was higher than than the pure PIL-Cl. This might be due to the hydrogen bonding interaction was introduced to the system by doping PIL-Cl, and as temperature rising, this interaction between PANI and PIL-Cl was broke. Moreover, the complex ratio for PIL-Cl and PANI could be calculated with the percentages of residuals at 450°C, and was showed in Table 2.

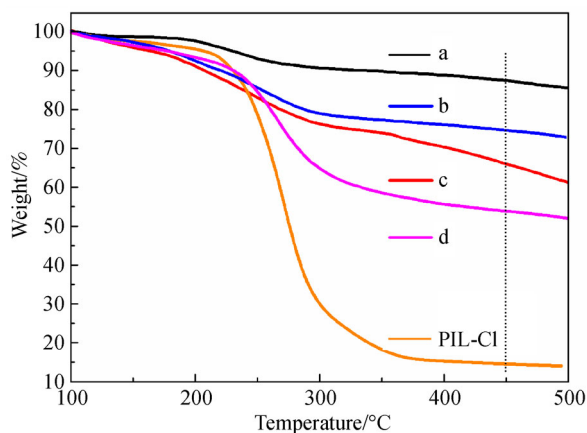


Fig. 6 TGA curves of pure (a) PANI, (b) PANIPIL1, (c) PANIPIL2 and (d) PANIPIL3.

3.5 Crystalline and conducting property of PANI doped by PILs

The XRD patterns of those formed PANIs were showed in Fig. 7. It was observed that the typical peaks of PANI were at 2θ 19.8° and 24.5°, representing a reflection plane of (020) and (200), respectively, corresponding to the amorphous structure of PANI [35]. In the XRD curves for the PIL-doped PANIs, the characteristic peak shifted slightly. Due to the periodicity parallel to the polymer chain, the peak at 19.8° shifted to 20.4°, and meanwhile, the peak shifted from 25.6° to 25.9° [36]. On the other hand, the shapes for the PIL-Cl doped composites were much the same as the pure PANI, indicating that the PIL-Cl doped PANIs preserved the pure PANIs' intact crystalline structure. The resistivity of PANIs doped by PIL-Cl was presented in Table 3. The PIL-Cl doped PANIs exhibited lower conductivity than the pure PANI. Furthermore, the resistivity became higher as the complex ratio of PIL-Cl in the PANIPILs increased.

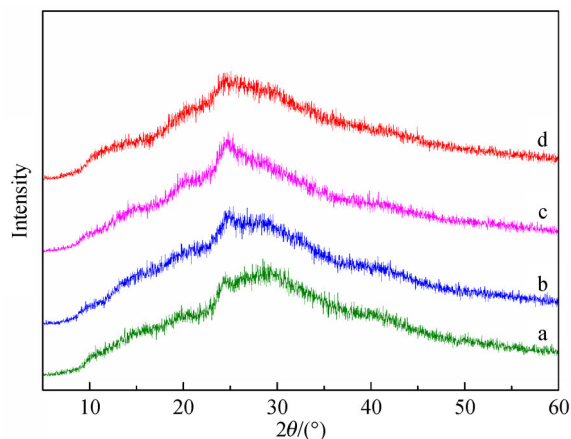


Fig. 7 XRD spectra of pure (a) PANI, (b) PANIPIL1, (c) PANIPIL2 and (d) PANIPIL3.

Table 3 Resistivity of the pure PANI and PANIs doped by PIL-Cl

Samples	Resistivity/($\Omega \cdot \text{mm}$)
PANI	134
PANIPIL1	136
PANIPIL2	697
PANIPIL3	3002

3.6 Introducing graphene in the polymerization of PANI

To increase the conductivity of soluble PANIs, we introduced the two dimensional conducting material graphene into the synthesis of soluble PIL-doped PANI. According to our previous research, graphene could be

dispersed well in water with the assistance PIL-Cl owing to the cation- π interaction [37]. Thus, referring to the fabrication procedure of PANIPI1 (the best solubility of all samples in several solvents), the same weight of graphene as PANI was added during the polymerization, and the product obtained was named PANIPI-G. The TEM image in Fig. 8 demonstrated that PANI uniformly distributed on the graphene which was in apparently contrast to the clean surface of the pure graphene. Benefitting from the cation- π interaction between the PIL-Cl and both PANI and graphene, the PIL-Cl acted as the bond between PANI and graphene which made the PANI attaching to the graphene sheet during the polymerization [18]. The chemical structures of PANI and graphene were characterized and confirmed by Raman and FTIR (supporting information). At the meantime, the one-dimensional radially aligned nanofiber structure of PANI remained. As shown in Fig. 9, the PANIPI-G could be well dispersed in several solvents indicating good solubility. The resistivity decreased apparently according to Table 4. This was because that the two-dimension graphene acted as a connection between the individual PANIs nanofiber, making them easy to conduct the current. As a result, the conductive network became denser and the conductivity increased. It can be concluded that introducing graphene during the polymerization didn't affect the dispersion of PANI/PIL, meanwhile it can enhanced the conductivity.

Table 4 Resistivity of the PANI, PANIPI1 and PANIPI-G

Samples	Resistivity/($\Omega \cdot \text{mm}$)
PANI	134
PANIPI1	136
PANIPI-G	17

4 Conclusions

In this study, polyaniline were synthesized in inorganic acids aqueous solution by chemical oxidation polymer-

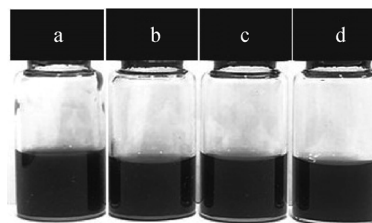


Fig. 9 Solubility experiments of PANIPI-G dispersed in (a) H_2O , (b) DMSO, (c) DMAc and (d) DMF.

ization with aniline as monomer and ammonium persulfate as oxidant. An imidazolium-based PIL-Cl was expected to serve as an unique dopant to afford protons for doping PANI and donate functional groups which can be incorporated onto PANI via π - π interaction, resulting in enhanced solubility. By doped with PIL-Cl, PANI could be dispersed well in water, DMSO, DMAc and DMF while the pure PANI could not. Meanwhile, too much the PIL-Cl composed with PANI will influence the conductivity negatively.

Acknowledgements The authors gratefully acknowledge the valuable help and great support from the Fundamental Research Funds for the Central Universities (Nos. 2232018D3-07, 2232018D3-24 and 2232019G-02), China Postdoctoral Science Foundation (No. 2016M591573), the National Natural Science Foundation of China (Grant No. 21404024) and Changsha Science and Technology Project. The project was funded by State Key Laboratory for Modification of Chemical Fibers and Polymer Materials, Donghua University.

Electronic Supplementary Material Supplementary material is available in the online version of this article at <https://doi.org/10.1007/s11705-020-1916-y> and is accessible for authorized users.

References

- Jacobo S E, Apesteguy J C, Anton R L, Schegoleva N N, Kurlyandskaya G V. Influence of the preparation procedure on the properties of polyaniline based magnetic composites. *European Polymer Journal*, 2007, 43(4): 1333–1346

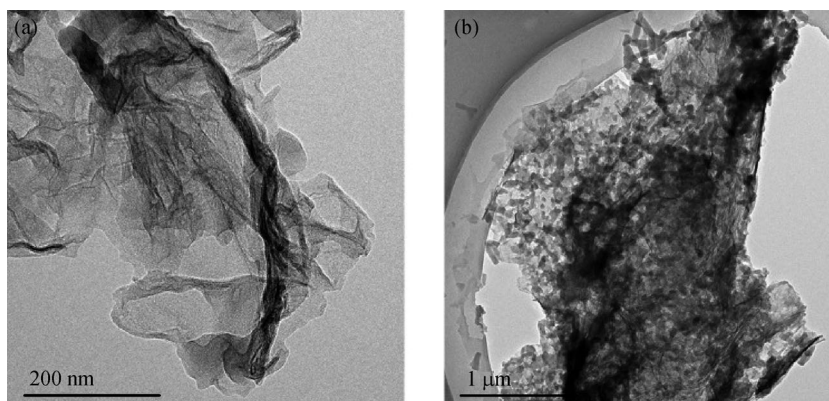


Fig. 8 TEM image of (a) the pure graphene and (b) the graphene/PANI composites.

- Bai S L, Zhao Y B, Sun J H, Tian Y, Luo R X, Li D Q, Chen A F. Ultrasensitive room temperature NH₃ sensor based on a graphene-polyaniline hybrid loaded on PET thin film. *Chemical Communications*, 2015, 51(35): 7524–7527
- Wang L L, Huang H, Xiao S H, Cai D P, Liu Y, Liu B, Wang D D, Wang C X, Li H, Wang Y R, Li Q, Wang T. Enhanced sensitivity and stability of room-temperature NH₃ sensors using core-shell CeO₂ nanoparticles@cross-linked PANI with *p-n* heterojunctions. *ACS Applied Materials & Interfaces*, 2014, 6(16): 14131–14140
- Hino T, Namiki T, Kuramoto N. Synthesis and characterization of novel conducting composites of polyaniline prepared in the presence of sodium dodecylsulfonate. *Synthetic Metals*, 2006, 156(21): 1327–1332
- Fahmy A, Eisa W H, Yosef M, Hassan A. Ultra-thin films of poly (acrylic acid)/silver nanocomposite coatings for antimicrobial applications. *Journal of Spectroscopy*, 2016, 5: 1–11
- Anisha B S, Biswas R, Chennazhi K P, Jayakumar R. Chitosan-hyaluronic acid/nano silver composite sponges for drug resistant bacteria infected diabetic wounds. *International Journal of Biological Macromolecules*, 2013, 62(11): 310–320
- Nateghi M R, Shateri-Khalilabad M. Silver nanowire-functionalized cotton fabric. *Carbohydrate Polymers*, 2015, 117(1): 160–168
- Palaniappan S, John A. Polyaniline materials by emulsion polymerization pathway. *Progress in Polymer Science*, 2008, 33(7): 732–758
- Patil A O, Heeger A J, Wudl F. Optical properties of conducting polymers. *Chemical Reviews*, 1988, 88(1): 183–200
- Bilal S, Gul S, Holze R, Shah A H A. An impressive emulsion polymerization route for the synthesis of highly soluble and conducting polyaniline salts. *Synthetic Metals*, 2015, 206: 131–144
- Cao Z F, Xia Y Q, Chen C. Fabrication of novel ionic liquids-doped polyaniline as lubricant additive for anti-corrosion and tribological properties. *Tribology International*, 2018, 120: 446–454
- Urbach B, Korbakov N, Bar-David Y, Yitzchaik S, Sa'Ar A. Composite structures of polyaniline and mesoporous silicon: Electrochemistry, optical and transport properties. *Journal of Physical Chemistry C*, 2007, 111(44): 16586–16592
- Harlev E, Gulakhmedova T, Rubinovitch I, Aizenshtein G. A new method for the preparation of conductive polyaniline solutions: Application to liquid crystal devices. *Advanced Materials*, 1996, 8(12): 994–997
- Dong J Q, Shen Q. Enhancement in solubility and conductivity of polyaniline with lignosulfonate modified carbon nanotube. *Journal of Polymer Science. Part B, Polymer Physics*, 2010, 47(20): 2036–2046
- Ayad M, El-Hefnawy G, Zaghlol S. Facile synthesis of polyaniline nanoparticles; its adsorption behavior. *Chemical Engineering Journal*, 2013, 217(2): 460–465
- Kinlen P J, Frushour B G, Ding Y, Menon V. Synthesis and characterization of organically soluble polyaniline and polyaniline block copolymers. *Synthetic Metals*, 1999, 101(1): 758–761
- Wang Y, Chen K, Li T, Li H M, Zeng R C, Zhang R L, Gu Y J, Ding J X, Liu H Q. Soluble polyaniline nanofibers prepared via surfactant-free emulsion polymerization. *Synthetic Metals*, 2014, 198: 293–299
- Calheiros L F, Soares B G, Barra G M O, Livi S. Ionic liquid—assisted emulsion polymerization of aniline in organic medium. *Materials Chemistry and Physics*, 2016, 179: 194–203
- Cao Y, Smith P, Heeger A J. Counter-ion induced processibility of conducting polyaniline and of conducting polyblends of polyaniline in bulk polymers. *Synthetic Metals*, 1992, 48(1): 91–97
- Ho K. Effect of phenolic based polymeric secondary dopants on polyaniline. *Synthetic Metals*, 2002, 126(2): 151–158
- Ouyang J. Recent advances of intrinsically conductive polymers. *Acta Physico-Chimica Sinica*, 2018, 34(11): 1211–1220
- Deb K, Sarkar K, Bera A, Debnath A, Saha B. Coupled polaron-electron charge transport in graphite functionalized polyaniline on cellulose: Metal free flexible *p*-type semiconductor. *Synthetic Metals*, 2018, 245: 96–101
- Yuan J, Antonietti M. Poly(ionic liquid)s: Polymers expanding classical property profiles. *Polymer*, 2011, 52(7): 1469–1482
- Yuan J, Mecerreyes D, Antonietti M. Poly(ionic liquid)s: An update. *Progress in Polymer Science*, 2013, 38(7): 1009–1036
- Marcilla R, Curri M L, Cozzoli P D, Martínez M T, Loinaz I, Grande H, Pomposo J A, Mecerreyes D. Nano-objects on a round trip from water to organics in a polymeric ionic liquid vehicle. *Small*, 2006, 2(4): 507–512
- Schüler D, Kerscher B, Beckert F, Thomann R, Mühlaupt R. Hyperbranched polymeric ionic liquids with onion-like topology as transporters and compartmentalized systems. *Angewandte Chemie International Edition*, 2013, 52(1): 455–458
- Bellayer S, Gilman J W, Eidelman N, Bourbigot S, Flambard X, Fox D M, Long H C, Trulove P C. Preparation of homogeneously dispersed multiwalled carbon nanotube/polystyrene nanocomposites via melt extrusion using trialkyl imidazolium compatibilizer. *Advanced Functional Materials*, 2010, 15(6): 910–916
- Kim T Y, Lee H W, Kim J E, Suh K S. Synthesis of phase transferable graphene sheets using ionic liquid polymers. *ACS Nano*, 2010, 4(3): 1612–1618
- Zhao H L, Yu Y T, Li Z H, Luo B, Wang X H, Wang Y P, Xia Y M. Linear polymeric ionic liquids as phase-transporters for both cationic and anionic dyes with synergic effects. *Polymer Chemistry*, 2015, 6(39): 7060–7068
- Fabio R, Do N G M, Santos P S. Dissolution and doping of polyaniline emeraldine base in imidazolium ionic liquids investigated by spectroscopic techniques. *Macromolecular Rapid Communications*, 2010, 28(5): 666–669
- Calheiros L F, Soares B G, Barra G M O, Livi S. Ionic liquid-assisted emulsion polymerization of aniline in organic medium. *Materials Chemistry and Physics*, 2016, 179: 194–203
- Zhang K, Zhang L L, Zhao X S, Wu J. Graphene/polyaniline nanofiber composites as supercapacitor electrodes. *Chemistry of Materials*, 2010, 22(4): 1392–1401
- Pernak J, Smiglak M, Griffin S T, Hough W L, Wilson T B, Pernak A, Zabielska-Matejuk J, Fojutowski A, Kitad K, Rogers R D. Long alkyl chain quaternary ammonium-based ionic liquids and potential applications. *Green Chemistry*, 2006, 8(9): 798–806
- Vaidya S G, Rastogi S, Aguirre A. Surfactant assisted processable organic nanocomposite dispersions of polyaniline-single wall carbon nanotubes. *Synthetic Metals*, 2010, 160(1): 134–138

35. Pouget J P, Jozefowicz M E, Epstein A J, Tang X, MacDiarmid A G. X-ray structure of polyaniline. *Macromolecules*, 1991, 24(3): 779–789
36. Zhang Z, Wan M, Wei Y. Highly crystalline polyaniline nanostructures doped with dicarboxylic acids. *Advanced Functional Materials*, 2010, 16(8): 1100–1104
37. Fu X Z, Liang Y, Wu R T, Shen J H, Chen Z D, Chen Y W, Wang Y P, Xia Y M. Conductive core-sheath calcium alginate/graphene composite fibers with polymeric ionic liquids as an intermediate. *Carbohydrate Polymers*, 2019, 206: 328–335